Peter VIRTIČ[1]

University of Maribor, Faculty of Energy Technology (1)

Determining losses and efficiency of axial flux permanent magnet synchronous motor

Abstract. *This paper presents the method for determining losses and efficiency of small axial flux permanent magnet synchronous motor with surface mounted permanent magnets and double external rotor by using measurements. Losses and efficiency are calculated by using measured electrical input power and mechanical output power. The characteristics obtained by the measurements are in good agreement with analytically calculated results and the results obtained by the finite element method.*

Streszczenie. W artykule opisano metodę pomiarowego wyznaczania strat oraz sprawności dla osiowo-strumieniowego silnika synchronicznego z magnesami trwałymi o małej mocy z magnesami montowanymi powierzchniowo i dwustronnym wale. Szukane parametry obliczane są na podstawie pomiarów wielkości elektrycznych wejściowych i mechanicznej mocy wyjściowej. Otrzymane charakterystyki porównano m. in. z wynikami analizy metodą elementów skończonych. (Określanie strat i sprawności osiowo-strumieniowego silnika synchronicznego z magnesami trwałymi).

Keywords: losses, efficiency, axial flux permanent magnet synchronous motor, measurement
Słowa kluczowe: straty, sprawność, osiowo-strumieniowa maszyna synchroniczna z magnesami trwałymi, pomiar.

Introduction

The rational use of energy became very important issue not only from the economic point of view but also from sustainability aspect. Many different approaches for determination of electrical machines losses and efficiencies have been published [1-5].

Diameter of the active part of the motor is 60 mm. Fig. 1 presents the configuration of AFPMSM and Fig. 2 its frequency converter.

Fig.1. Prototype AFPMSM: a) housing, b) active part placed in the housing, c) structure of the active part, d) active part with stator winding and rotor

This paper presents measured and calculated characteristics of prototype axial flux permanent magnet synchronous machine (AFPMSM) of smaller dimensions which operates as a motor. The main focus of this paper is to present the procedure of determining losses and efficiency of AFPMSM by using measurements.
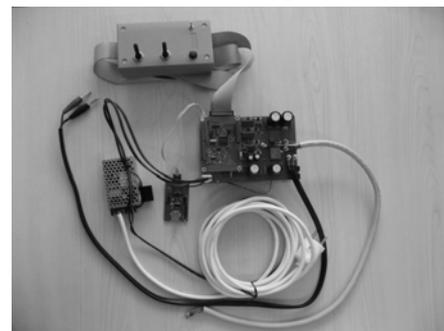
Fig.2. Frequency converter for AFPMSM

AFPMSM characteristics including power losses and efficiency are measured by using experimental setup presented in Fig. 3.
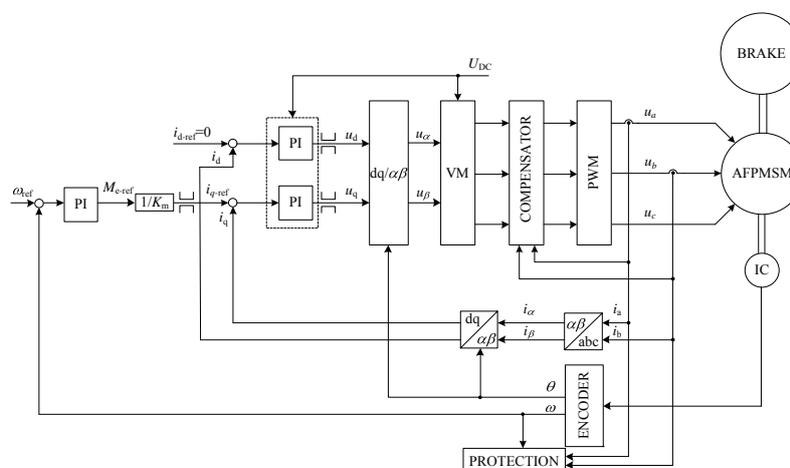
Fig.3. Scheme of the experimental setup

Measurement method

In the experimental system the power supply of AFPMSM is implemented by using the frequency converter and the load is carried out with the passive brake with double bearing housing. On the other side of AFPMSM shaft the incremental counter (IC) is mounted. All other elements of the experimental system presented in Fig. 3 are implemented in the frequency converter (Fig. 2), which was made out for the needs of the prototype AFPMSM. The motor power supply consists of the MOSFET transistors which, together with capacitors, present the power section of the frequency converter. With one of the potentiometers in Fig. 2 the reference value of rotor speed can be changed. In the feedback loop the incremental counter (IC) and rectangular pulse encoder, which converts the pulses from the IC to the angle and angular velocity, are in the series connection. With the second potentiometer the electric current can be limited due to the safety reasons. In order to control the angular velocity of the AFPMSM the PI controller is used and taking into account the torque constant (K_m) the reference value of current component q is defined. PI controller of the current in the dynamic control take into account the voltage (U_{DC}) of DC intermediate circuit. After dq/αβ transformation follows the voltage vector modulation (VM) and further the compensation of the load impact. The protection to exclude the power converter in case of excessive increases in the current or rotor rotational speed is also carried out. The maximum available voltage in the DC intermediate circuit is limited to 90 V by the algorithm, which protects the MOS-FET transistors. The maximum allowed peak current to supply the motor is 20 A.

Before the measurements of AFPMSM characteristics in the motor mode began the open circuit back electromotive force (EMF) waveform depending on the position of the rotor was measured at no-load condition and 2400 rpm, which is also the maximum speed of prime mover of the experimental setup. Measured phase back EMF waveforms were compared with the waveforms calculated by using the analytical method and finite element method (FEM) (Fig. 4).
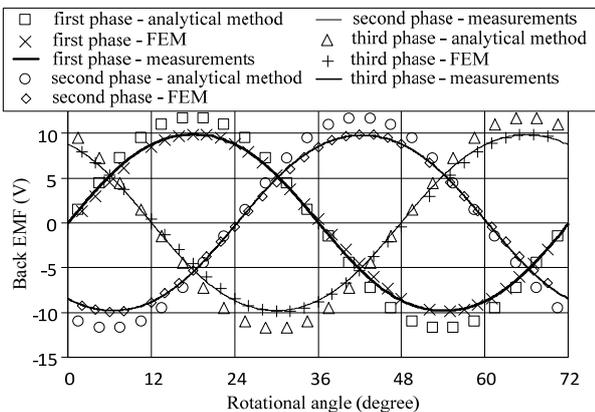
Fig.4. Comparison between calculated and measured results of back EMF waveforms according to displacement at 2400 rpm

Measured results and discussion

This section presents measured characteristics of the prototype AFPMSM of smaller dimensions in the motor mode. For each load and speed of the rotor of AFPMSM the average terminal voltage of all three phases is presented in Fig. 5. Terminal voltage of the AFPMSM increases with increasing the load and rotor speed of AFPMSM. Because of the upper limit 90 V of DC intermediate circuit this circuit is fed by DC voltage of 83 V.

In the case where the AFPMSM supply voltage is pure sinusoidal or at least very close to sinusoidal form the first approximation of phase to phase RMS voltage can be calculated by using the equation (1).

$$（1）\qquad U_{DC} = \sqrt{2}U = \sqrt{2}\sqrt{3}U_{ph}$$

where: U_{DC} – DC intermediate circuit voltage, U – phase to phase RMS voltage, U_{ph} – phase RMS voltage.

If the equation (1) is used and the DC voltage of DC intermediate circuit is 83 V, the RMS phase to phase voltage is 59 V and RMS phase voltage is 34 V, which is also evident from the measured voltage in Fig. 5.

For more accurate determination of the voltage at the output of the converter the voltage drops in the transistors should be considered. Due to the limitation in increasing the voltage, the torque load increase causes the rotational speed lowering despite the constant reference rotational speed. In general, the higher rotational speed requires higher output voltage of the frequency converter. Therefore, at higher rotational speeds the highest possible value of output voltage, that the converter is capable to achieve, will be at lower loads.
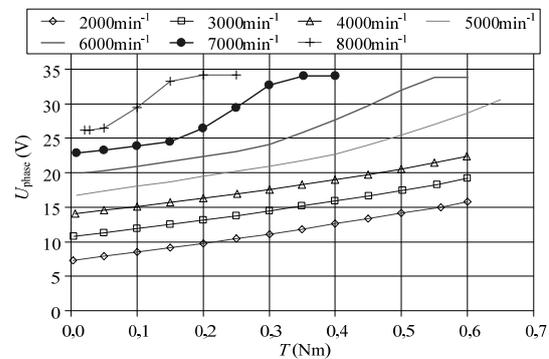
Fig.5. Average RMS phase voltages for individual torques at different reference rotor speeds

Figure 6 presents the average RMS current value of all three phases as a function of load torque at different reference rotational speeds. When the voltage exceeds certain value (Fig. 5), the current begins to rise even faster with a further increase of the load torque (Fig. 6). The higher is the rotational speed, lower is the load where the current starts to rise rapidly. At lower rotational speeds, when the converter has high enough voltage available, the relationship between current and torque is linear.
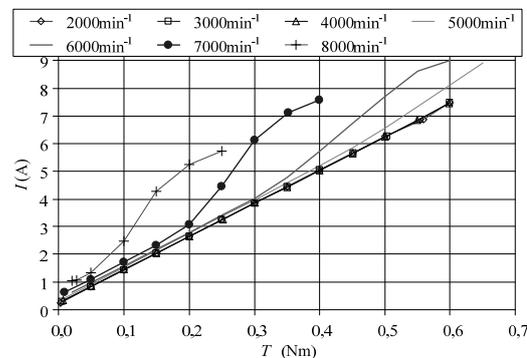
Fig.6. Measured RMS load current as a function of torque at different reference rotor speeds

Individual values of the currents in Fig. 6 correspond to the current densities presented in Fig. 7. At selected nominal current 4 A the current density is 7,07 A/mm².
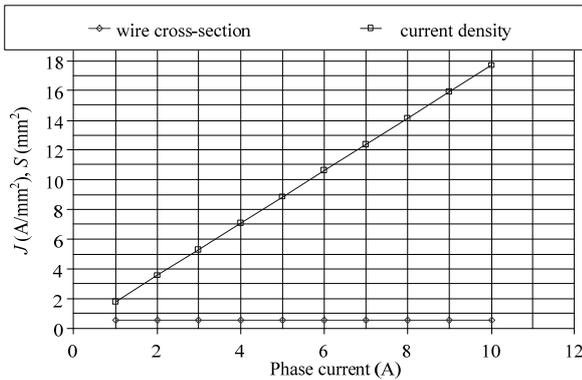
Fig.7. Presentation of the wire cross-section and current densities in the winding of AFPMSM in dependency on the current

Fig. 8 presents the comparison between the static torque characteristics calculated by FEM and analytical method via magnetic vector potential. Both calculated characteristics are in good agreement. In Table 1 the comparison of peak values calculated by the analytical method and FEM shows good agreement with measured torque at the current of 4 A, with the exception of the cases (at higher reference rotational speeds) where the limitation of voltage in the frequency converter affects the measured results.
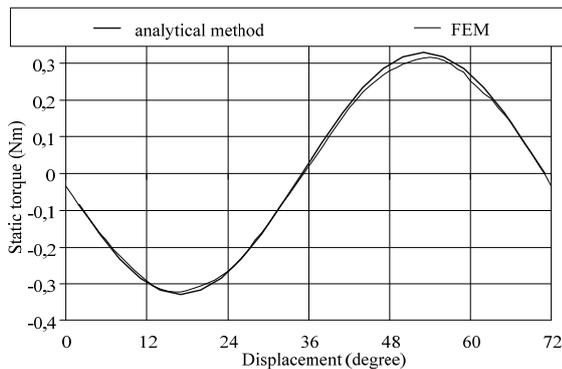
Fig.8. Static troque calculated by analytical method and FEM

Table 1. Comparison between calculated and measured torque at load current of 4 A

	Rotational speed (rpm)	Analytical method	FEM	Measured results
Torque (Nm)	3000	0,329	0,316	0,313
	4000	0,329	0,316	0,313
	5000	0,329	0,316	0,301
	6000	0,329	0,316	0,298
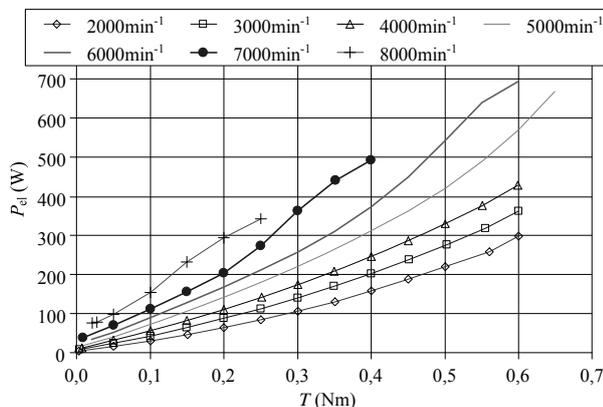
Fig.9. Measured electrical input power in dependency on torque at different reference rotor speeds

Even when we observe the input electric power in dependency on the load torque, we come to the conclusion that the characteristics of electric power at higher rotational speeds deviate from the trend of rising power as a function of load torque at lower reference rotational speed (Fig. 9).

As expected, the mechanical power on the AFPMSM shaft is higher at higher rotational speeds (Fig. 10) and by taking into account the equation (2) we can calculate the losses in dependency on the load (Fig. 11).

$$(2) \qquad P_{\text{loss}} = P_{\text{el}} - P_{\text{m}}$$
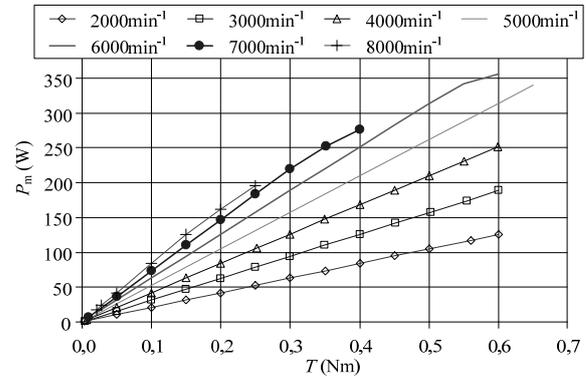
Fig.10. Measured power on the shaft in dependency on torque at different reference rotor speeds
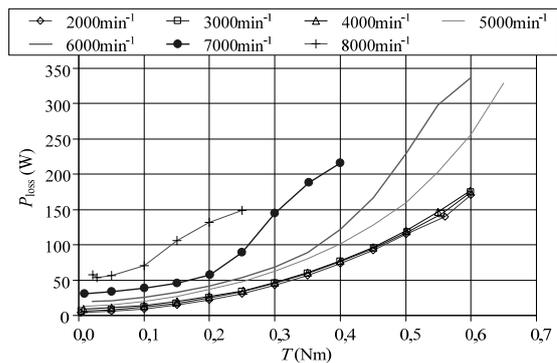
Fig.11. Measured power losses in dependency on torque at different reference rotor speeds

Figure 12 presents the comparison between measured losses and losses calculated in the copper due to current load. Losses in the rotor iron are neglected due to the large equivalent air-gap and very small variation of the magnetic field in the massive rotor discs. Due to the coreless stator there are no iron losses.
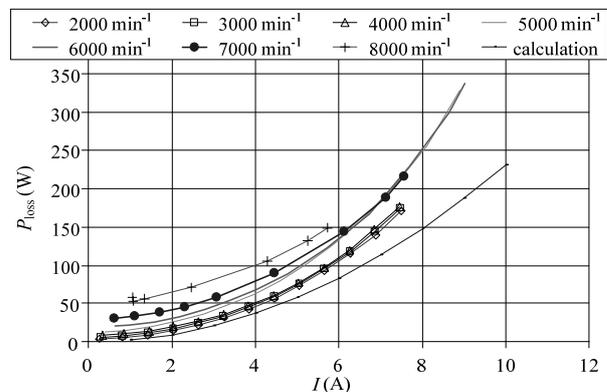
Fig.12. Measured power losses in dependency on current at different reference rotor speeds and comparison with calculated losses in the copper

The efficiency is determined by using the equation (3) and presented in Fig. 13.

$$(3) \qquad \eta = \frac{P_{\mathrm{m}}}{P_{\mathrm{el}}}$$
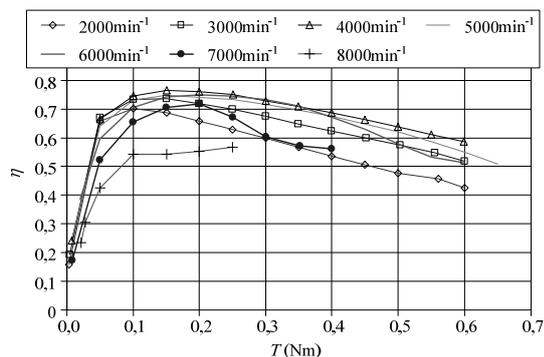
Fig.13. Efficiency in dependency on torque at different reference rotor speeds

Measured power factor characteristics as a function of load torque at different reference rotor speeds are shown in Fig. 14, where the influence of limited converter output voltage is expressive and the converter can no longer maintain the constant rotor speed of AFPMSM.
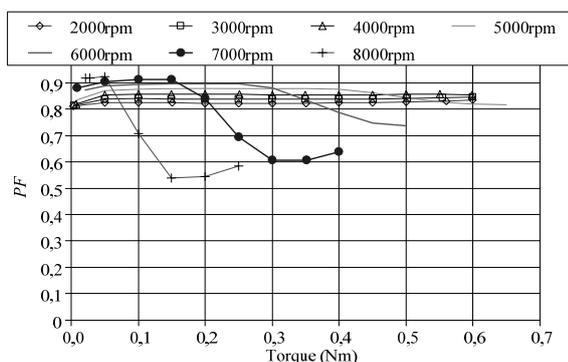
Fig.14. Power factor in dependency on the load torque at different reference rotational speeds

Conclusion

As it can be seen in Fig. 13 it is clear that the efficiency is reaching maximum at 4000 rpm. Due to converter voltage limit the efficiency is significantly reduced at 8000 rpm and the losses are increased (Fig. 12).

Calculated and measured results of back EMF waveforms according to displacement at 2400 rpm are in good agreement. Figure 4 presents the deviation of analytically calculated back EMF because the influence of the active machine part edge is not taken into account during the calculation.

REFERENCES
[1] Hadziselimovic M., Marcic T., Stumberger B. and Zagradisnik I., Winding type influence on efficiency of an induction motor, *Prz. Elektrotech*., 87 (2002), no. 3, 61-64
[2] Stumberger, B., Hamler A., Gorican V., Jesenik M. and Trlep M., Accuracy of iron loss estimation in induction motors by using different iron loss models, *Journal of Magnetism and Magnetic Materials*, 272 (May 2004), Suppl. 1, 1723-1725
[3] Štumberger B., Goričan V., Štumberger G., Hamler A., Trlep M., Jesenik, M., Accuracy of iron loss calculation in electrical machines by using different iron loss models, *Journal of Magnetism and Magnetic Materials*, 254/255 (2003), 269-271
[4] Marcic, T., Stumberger B. Stumberger G., Hadziselimovic M.; Zagradisnik I., The impact of different stator and rotor slot number combinations on iron losses of a three-phase induction motor at no-load, *Journal of Magnetism and Magnetic Materials*, 320 (Oct. 2008), no. 20, 891-895
[5] Stumberger B., Hamler, A., Hribernik B., Analysis of iron loss in interior permanent magnet synchronous motor over a wide-speed range of constant output power operation, *IEEE Trans. Magn.*, 36 (July 2000), no. 4, 1846-1849
[6] Gieras J.F., Wang R.J. and Camper M.J., Axial flux permanent magnet brushless machines, *Kluwer Academic Publishers*, Dordrecht, 2004

Authors: *asst. prof. Peter Virtič, Ph.D., University of Maribor, Faculty of Energy Technology, Hočevarjev trg 1, 8270 Krško, E-mail: peter.virtic@uni-mb.si.*